Reaction Kinetics, Mechanisms and Catalysis (2022) 135:1423–1437
https://doi.org/10.1007/s11144-022-02209-7

Synthesis, characterization and kinetics of sustained pantoprazole release studies of interpenetrated poly(acrylic acid)-chitosan-bentonite hydrogels for drug delivery systems

Vesna Teofilović[1] · Busra Agan[2] · Jelena Pavličević[1] · Davut Lacin[3] · Ayse Zehra Aroguz[2]

Received: 22 December 2021 / Accepted: 23 March 2022 / Published online: 10 April 2022

Abstract

Clays are widely used in controlled drug delivery systems due to their strong adsorption properties and natural origin. In this study, a drug carrier was prepared using chitosan, a natural polymer, mixed with bentonite clay. Then, poly(acrylic acid) was added to improve its swelling properties. Pantoprazole was chosen as the model drug. The swelling properties of the prepared samples were investigated at two different temperatures: 25 and 37 °C. The prepared samples were examined by Fourier-transform infrared spectroscopy and scanning electron microscopy. The controlled release of the pantoprazole from the drug carriers indicated that the release of the pantoprazole is temperature-sensitive. In order to study the effect of bentonite on the drug carrier system, drug release was also investigated in the samples without adding clay. It was observed that the drug release profiles of the prepared sample containing bentonite fitted better than the sample without clay. The release kinetics analysis showed that the first-order and the Korsmeyer-Peppas models fit the best, and that pantoprazole was transported via Fickian diffusion. The prepared samples showed the capability of pantoprazole loading and, thus, its possibility to be used in drug delivery systems.

Keywords Drug delivery systems · Drug release kinetics · Pantoprazole · Chitosan

✉ Vesna Teofilović
vesnateofilovic@uns.ac.rs

[1] Faculty of Technology Novi Sad, Bul. Cara Lazara 1, University of Novi Sad, 21000 Novi Sad, Serbia

[2] Engineering Faculty, Chemistry Department, Istanbul University-Cerrahpasa, 34320, Avcilar, Istanbul, Turkey

[3] Engineering Faculty, Department of Geological Engineering, Istanbul University-Cerrahpasa, 34320, Avcilar, Istanbul, Turkey

Introduction

Besides their therapeutic properties, most of the drugs have side effects. The extent of a negative impact can vary from person to person [1–3]. For this reason, the drug should be administered into the body in a controlled manner and in a precisely determined amount, which can vary depending on the conditions (temperature, pH) of the targeted area of the body [4]. In recent years, scientific studies on controlled drug release have been trending towards developing more efficient and novel controlled drug release systems [5, 6]. Various drug delivery-release techniques, such as smart mucoadhesive buccal patches [7], NIR-light–controlled drug release using polymeric hydrogels [8], adsorption of drug and coating process [9–11], pellet formation [12], core–shell technique [13], microbead preparation [14], electrospun fibers [15–18], 3D printing of medicines [19, 20] are widely studied. The latest generation of drug delivery systems includes nanorobots [21, 22], gene therapy [23, 24], and long-term delivery systems (6–12 months) [25, 26].

Since drug delivery systems have to be biocompatible, biopolymers and other natural substances such as clays are preferably used as drug carrier materials [27, 28]. Properties of clays, such as high adsorption capacity, chemical inertness, thixotropy, specific surface area, ion exchange capacity, less toxicity for oral administration, high swelling, can help in enhancing the physicochemical and organoleptic characteristics of drugs and their delivery systems [29]. In particular, the adsorption capacity of clays plays an important role in drug carrier systems [30]. To successfully incorporate layers of clay into biopolymers for drug delivery systems, clay-polymer hybridization is usually done via one of four methods: in situ synthesis, solution intercalation, in situ intercalative polymerization, and melt intercalation [31]. Such a system has been reported by Nizam el-Din and Ibraheim, where they produced nanocomposite hydrogels by gamma-radiation copolymerization of acrylic acid (AAc), by adding montmorillonite (MMT) as a clay mineral and chitosan as a biopolymer. They showed that the swelling of the sample increased by adding MMT into the hydrogel [28]. In addition, clays have a high-energy hydrophilic surface. For this reason, they cannot be readily incorporated into a hydrophobic polymer matrix. To achieve compatibility with polymers, hydrophilic clay should be made organophilic by ion-exchange reactions using organic cations such as alkylammonium ions. As a result of the ion-exchange reaction, the distance between the layers of the clay increases, and the surface is modified to become polymer-compatible i.e. organophilic [32].

Various parameters influence the release of the drugs such as pH, their quantity and temperature. Chitosan is a biodegradable, natural polymer, and is widely used in many scientific studies in pharmaceutical and medical fields due to its non-toxicity and biocompatibility [33]. Several studies within the literature report the preparation of drug carriers by mixing polymers with various clays [28–30, 34–37]**.** It is known that clay addition delays the biodegradation (for a limited period) of biopolymers prepared as drug carriers. Lin et al. synthesized and characterized the chitosan/organoclay bionanocomposites by mixing chitosan in acetic acid with montmorillonite [34].

Chitosan and acrylic acid are preferred in controlled drug release systems as the compatible polymers for various drugs. Wang et al. studied chitosan—poly(acrylic acid) crosslinked hydrogels to control the amoxicillin and meloxicam drug release via pH. They found that the rates of drug release from the loaded hydrogels increased with an increase in pH [38]. They showed that Korsemeyer-Peppas and Weibull models fitted drug release data, and the results indicated that the prepared materials provided an ideal basis for controlled drug delivery and release systems. Furthermore, biodegradable N-succinyl chitosan-g-poly (acrylic acid) hydrogels were prepared by Bashir et al. and they used their prepared samples to carry theophylline in-vitro where the latter is used for the treatment of asthma [39].

In an aqueous environment, bentonite disperses to form a colloidal solution, when coupled with polymerous materials. However, there isn't enough research reported within the literature in regard to their use in drug release systems.

Pantoprazole, selected as a model drug, is used as a proton pump inhibitor to reduce gastric acidity in Gastro-oesophageal reflux disease and also heal gastric and duodenal ulcers. Controlled use of pantoprazole is very important due to side effects such as headache, diarrhea, flatulence, and abdominal pain [40, 41].

The main aim of this work is to decrease the swelling ratio of poly(acrylic acid)/chitosan/clay hydrogel by adding clay and prolonging the drug release time, sequentially improving the drug efficacy by introducing clay. For this purpose, bentonite clay was added to the poly(acrylic acid)/chitosan biopolymer. Drug loading and release of the biomaterial were studied using a pantoprazole drug active agent. The pantoprazole release kinetics was examined using various kinetic equations. The successful results were obtained for the first-order and the Korsmeyer-Peppas kinetic models.

Materials and methods

Preparation and modification of the clay

Bentonite clay was obtained from Resadiye Province, Turkey. Cation exchange capacity (CEC) is 75 meq/100 g. The chemical structure of bentonite is: 57.1% SiO_2, 16.8% Al_2O_3, 2.6% Na_2O, 3.4% CaO, and 3.8% Fe_2O_3 and 15.2% loss on ignition (LOI) value, with a trace amount of impurities [42]. Before being used, bentonite was washed with distilled water to remove its impurities and water-soluble salts. Then, it was dried, ground, and sieved through a 125 mesh sieve. The clay was modified before adding into the prepared hydrogels, according to the literature [43, 44]. For this purpose, 0.5 g of clay was continuously stirred in 100 ml of 2% nitric acid solution for 2 h. Afterward, the clay was washed with water and centrifuged. Finally, the modified bentonite was dried at 80 °C until constant weight.

The preparation of drug carrier

The preparation of poly(acrylic acid)/chitosan (pAA-g-Chi)

0.5 g of chitosan (Aldrich) was dissolved in 30 ml of 1% acetic acid (Merck) solution in a two-necked flask. The dissolution process was also carried out in a water bath at 65 °C. 0.335 g of potassium peroxydisulfate (KPS) (Sigma-Aldrich), as the polymerization initiator, was added to the dissolved material to obtain a radical form. Then 3.35 g of acrylic acid (AA) was added with 1% N, N- methylene-bis-Acrylamide solution (Sigma-Aldrich) by continuously stirring for 1 h. The resulting solution was poured into a Teflon petri dish and dried in an oven at 50 °C until it reached a constant weight, and it is named as pAA-g-Chi. The dried sample was kept in a desiccator until used.

The preparation of poly(acrylic acid)/chitosan/clay (pAA-g-Chi-clay)

The sample coded as pAA-g-Chi-clay was prepared by adding modified clay to the mixture of pAA-g-Chi. For this purpose, 0.4 g of modified clay dispersed in 40 ml of distilled water was added to chitosan before mixing with acrylic acid and N, N- Methylene-bis-Acrylamide solution. Then, the obtained solution was poured into a Teflon petri dish, dried, and kept for the next usage.

The swelling behavior of pAA-g-Chi and pAA-g-Chi-clay samples was examined, and, the swelling ratio was calculated using the Eq. 1:

$$\text{Swelling}(\%) = \frac{W_s - W_d}{W_d} \times 100 \tag{1}$$

Here W_s is the weight of swollen sample at any time, and W_d is the weight of the dry composite.

Obtained samples were investigated for structural and morphological properties. For those purposes, Fourier-transform infrared spectroscope (FTIR) Thermo Nicolete IS-10 and scanning electron microscope (SEM) ZEISS EVO LS10, were used, respectively.

For the swelling experiments, 0.10 g of samples were used. The samples were kept in distilled water (pH = 6.5), for a certain time. Then, they were removed from the distilled water, the water excess was removed, and samples were weighed. Fig. 1 shows the pAA-g-Chi-clay sample before (a) and after swelling in distilled water after 30 min (b).

Drug loading and release studies

Drug loading and release studies of the active substance pantoprazole were conducted on the prepared samples.

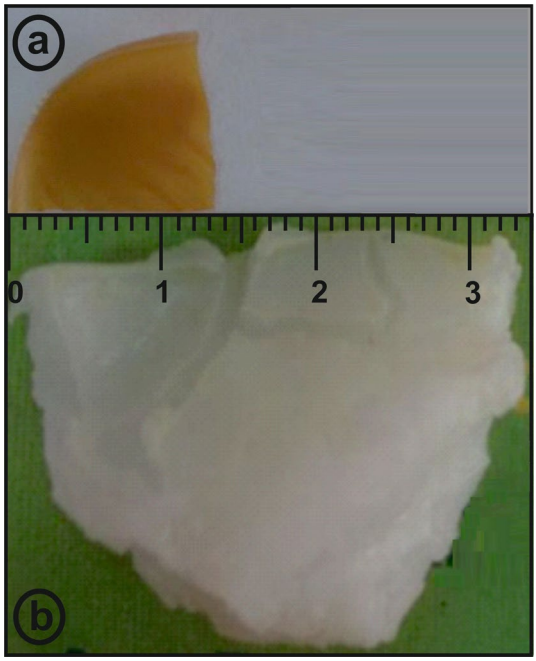

Fig. 1 The sample of poly(acrylic acid)/chitosan/clay: **a** dried sample and **b** swollen sample in distilled water at 25 °C after 30 min

Standard curve of pantoprazole and loading process

Absorbance values of pantoprazole were measured with a UV–Vis Spectrophotometer (T80 + UV/VIS PG Instruments double beam), at wavelength of 289 nm. For this purpose, a stock solution of 0.2 g/L of pantoprazole was prepared. Then, five different dilute solutions were obtained from the stock, with decreasing concentrations of 50, 25, 12.5, 6.25 and 3.125 mg/L, and their absorbance values were measured (Fig. 2). The standard curve equation for this graph was calculated to be $y = 28.236x – 0.0072$; with a high value of the coefficient of determination ($R^2 = 0.998$).

The linear relationship between the drug concentration and its absorbance values was obtained by adding the trendline to the standard graph in Fig. 2.

Pantoprazole active drug loading and release studies were performed on pAA-g-Chi-clay samples at two different temperatures. Pantoprazole was loaded into the prepared pAA-g-Chi-clay sample in distilled water at 25 °C until the constant weight.

The initial concentration of Pantoprazole solution was 0.085 g/L and the loading time was almost 4 h. The loading process was physical adsorption. The amount of pantoprazole loaded into the gel was determined from its decreasing concentration in the solution.

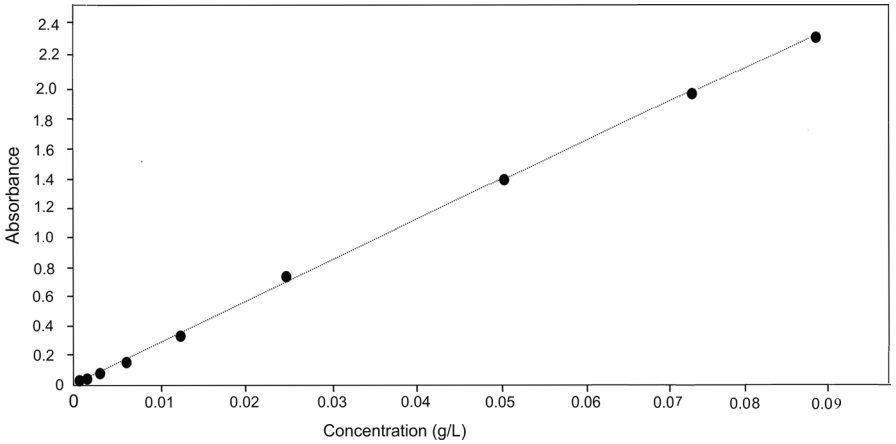

Fig. 2 Standard (calibration) curve of the pantoprazole active substance at 25 °C ($R^2 = 0.998$)

Study of the prepared pAA-g-Chi-Clay in controlled drug release systems.

Release studies of drug-loaded samples were carried out in distilled water with pH = 6.5 and buffer solutions with pH = 2.0 and pH = 7.6. The release of the drug in the buffer solution at pH = 7.6 was found to be very low (35%) when compared to the release in distilled water. The release of the drug in the buffer solution at pH = 2.0 was also carried out and it was observed that the percentage of the drug release in buffer solution at pH = 2.0 was very close to the drug release results in distilled water (100%). But, the release was very fast compared with the release in distilled water. Therefore, drug release studies were continued in distilled water afterward. The cumulative drug release was determined by using 0.085 g/L drug concentration as a reference for the release study. The loading capacity of the drug in the hydrogel was calculated from the remaining drug concentration in the solution.

Kinetic studies

The first-order kinetics model

As stated in Eq. 2, the first-order kinetic is expressed as an exponential function depending on concentration and time.

$$\left[C_t\right] = [C]_0 e^{-kt} \tag{2}$$

Here C_0 is the initial drug concentration and C_t is the concentration of the drug at any time. Parameter k_1 is the first-order rate constant.

Korsmeyer-Peppas kinetics model

Korsmeyer et al. (1983) described drug release from a polymeric system with a simple relationship [45]. The theories proposed by Korsmeyer–Peppas showed the ratio between the drug released amount (M_t) to the medium at any time t and the total drug released amount (M_1) can be approximated by the exponential expression given in Eq. 3.

$$F = \frac{M_t}{M_\infty} = K_m t^n \tag{3}$$

$M_t/M_{\infty:}$ is a drug release ratio at time t; K_m is kinetic constant and n is diffusion coefficient which is dependent on the drug release mechanism. In film tablets, $n < 0.5$ corresponds to a Fickian diffusion mechanism. Whereas, a value of $0.5 < n < 1.0$ indicates a non-Fickian diffusion and $n = 1$ indicates a super-diffusion [46, 47].

Results and discussion

The structural and morphological analyses of the prepared samples were performed by FTIR and SEM methods, respectively. Fig. 3 shows the comparison of FTIR spectra of pure chitosan and pAA-g-Chi sample, while the comparison of FTIR spectra of pure clay and pAA-g-Chi-clay sample is given in Fig. 4.

In Fig. 3, the overall shape of the two spectra appears to be similar. The characteristic peaks of chitosan are located at 3418 cm^{-1} belonging to hydroxyl group, and the absorption bands at 1644, 1531, 1383, 1090 cm^{-1} are assigned to C=O of amide I, N – H, amide III, C_3-OH, of Chi, respectively. The absorption bands of pAA are detected at around 3432 $cm^{-1}$and 1452 cm^{-1}. The peak at 3432 cm^{-1} appears as

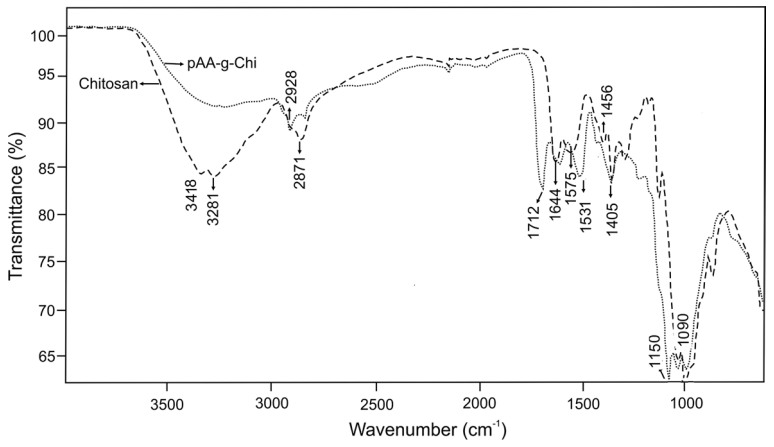

Fig. 3 FTIR spectra of pure chitosan and poly(acrylic acid)/chitosan sample

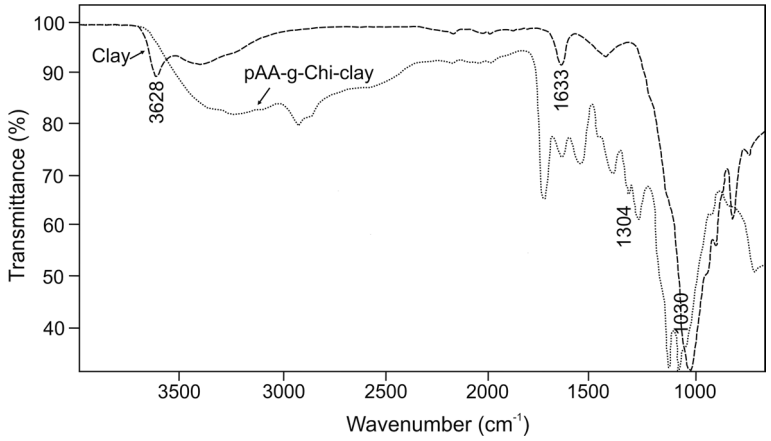

Fig. 4 FTIR spectra of clay and poly(acrylic acid)/chitosan/clay sample

a broad peak in the pAA-g-Chi compound and overlapps with the hydroxyl group of chitosan peak at 3418 cm^{-1} in the pAA-g-Chi sample. Also, due to the effect of graft polymerization with acrylic acid, the peak at 1575 cm^{-1}, corresponding to the $–NH_2$ groups within chitosan, is shifted to 1531 cm^{-1} whereas, the one detected at 1378 cm^{-1}, corresponding to the –OH groups, has completely disappeared. In the spectrum of Chi, however, the absorption bands at 1575 and 1090 cm^{-1} disappeared after the reaction with AA, as shown in spectra of pAA-g-Chi (Fig. 3) and pAA-g-Chi-Bentonite (Fig. 4), which reveals that both $-NH_2$ and $-OH$ groups of Chi took part in g-polymerization with AA. Fig. 4 shows FTIR spectra of clay-loaded pAA-g-Chi samples against pure clay. It can be seen that the peak corresponding to the H–O–H bending vibrations in the pure clay observed at 1633 cm^{-1} in the FTIR spectrum overlaps with the –NH peak at 1644 cm^{-1} and –COOH stretching vibration peak at 1712 cm^{-1} of non-clay-loaded pAA-g-Chi sample in Fig. 3. The peaks between 1000 and 792 cm^{-1} wavenumbers correspond to the –OH bending vibrations and Si–O vibrations found within the tetrahedral and octahedral structure of the clay. Si–OH vibration peak at around 1000 cm^{-1}, belonging to clay, is slightly shifted to the lower wavenumber value.

The new absorption band at 1405 cm^{1} (symmetric $-COO^{-}$ stretching) indicates the existence of pAA chains. As can be seen from the spectrum of pAA-g-Chi, the absorption band at 1644 cm^{-1} (C=O of amide I) was overlapped by C=O of $-$ COOH and asymmetric $-COO^{-}$ stretching. Mahdavinia et al. reported a similar result in the chi-*g*-p(AA-co-acrylamide) system [48].

Morphologic analysis of pAA-g-Chi and pAA-g-Chi-clay samples was assesed by SEM (Figs. 5 and 6), respectively. Fig. 5 shows the porous structure of the prepared pAA-g-Chi sample at two different magnifications (1000× and 5000×, respectively), while a smoother and more homogeneous structure of the clay-loaded sample is detected in Fig. 6.

The swelling behavior of the pAA-g-Chi samples, before and after bentonite addition, was examined at 25 °C, and the obtained results are presented in Fig. 7

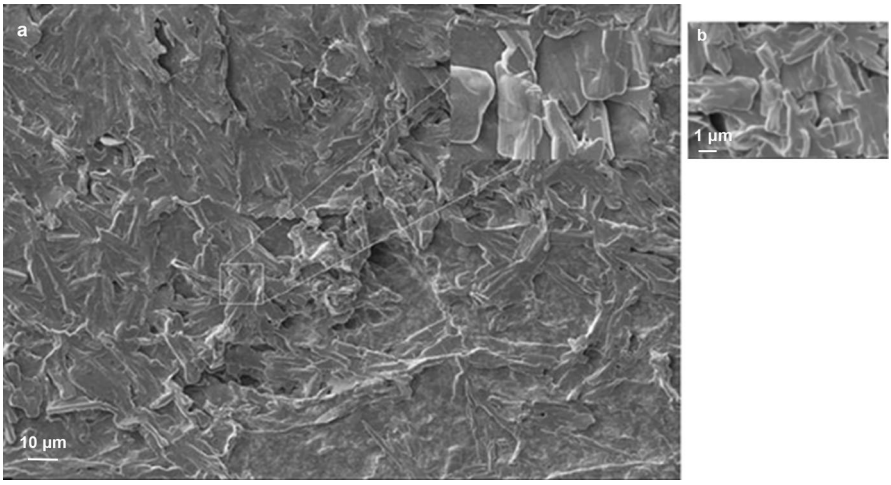

Fig. 5 SEM micrograph of the prepared poly(acrylic acid)/chitosan sample, at two different magnifications: **a** 1000× and **b** 5000×

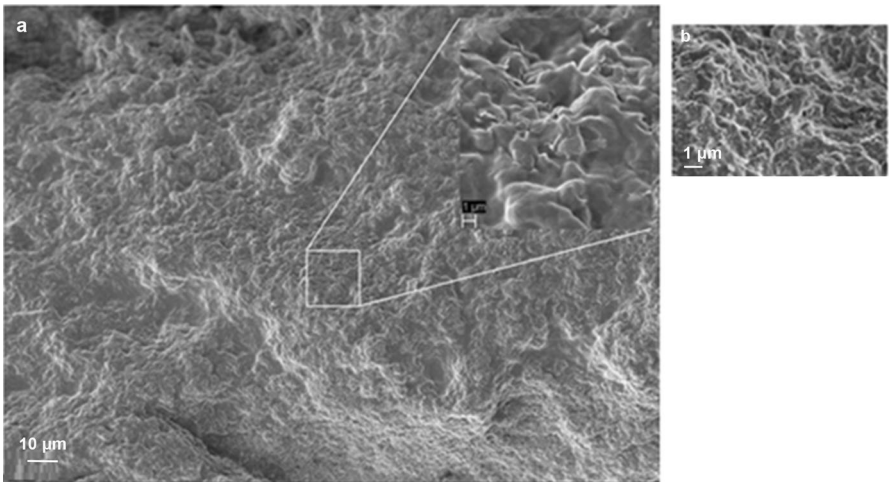

Fig. 6 SEM micrograph of the prepared poly(acrylic acid)/chitosan/clay sample at two different magnifications: **a** 1000× and **b** 5000×

It can be seen that bentonite addition slightly decreased the sample swelling. For both samples, the maximum swelling was achieved at around 30 min, where the sample of pAA-g-Chi-clay has reached equilibrium after 60 min. The sample containing clay showed a more stable structure. After reaching the maximum value, the dispersion was observed in the clay-free sample, while the pAA-g-Chi-clay sample was found to be more stable.

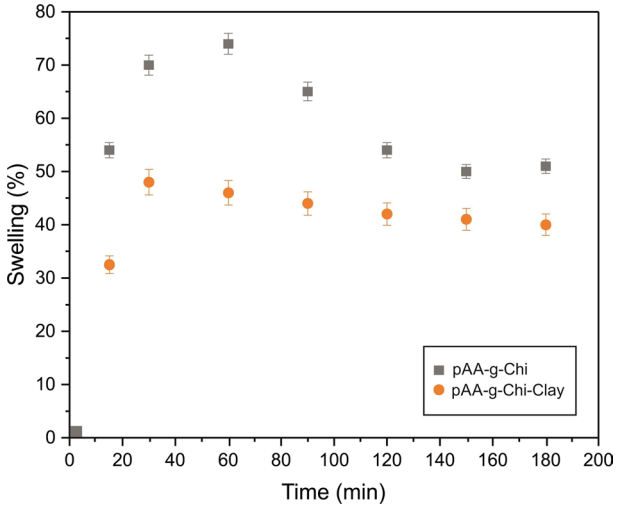

Fig. 7 Swelling behavior of the poly(acrylic acid)/chitosan samples, before and after the clay addition, in distilled water at 25 °C

Loading of the pantoprazole active substance

Fig. 8 shows the change in concentration of the pantoprazole that is being loaded on the prepared samples pAA-g-Chi and pAA-g-Chi-clay versus time. As seen from Fig. 8, the equilibrium reach of the drug loading process took almost 180 min for both samples (pAA-g-Chi and pAA-g-Chi-clay).

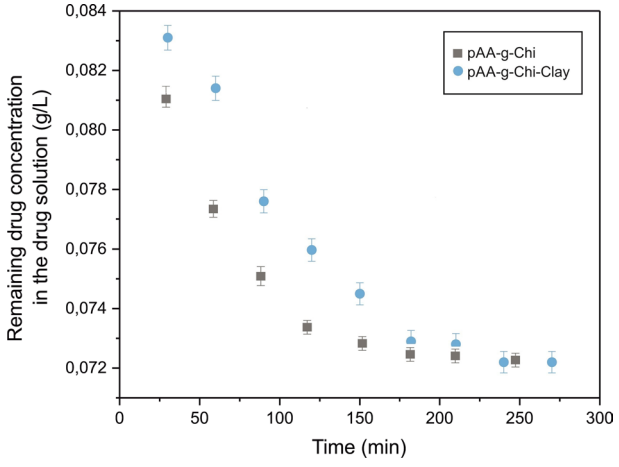

Fig. 8 Drug loading on the poly(acrylic acid)/chitosan/clay, at 25 °C

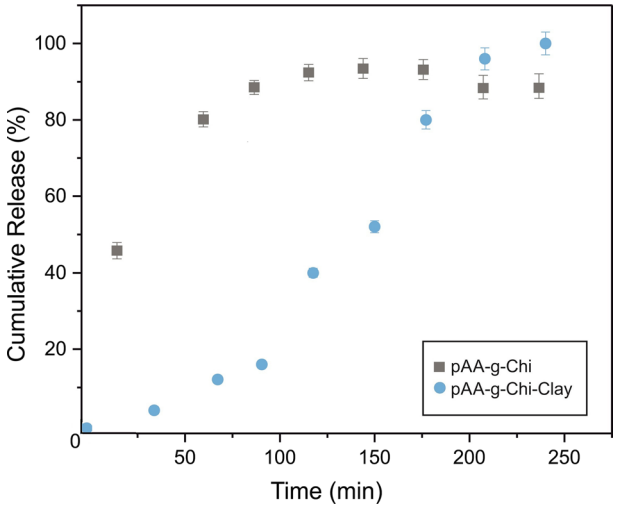

Fig. 9 Drug release in distilled water at 25 °C

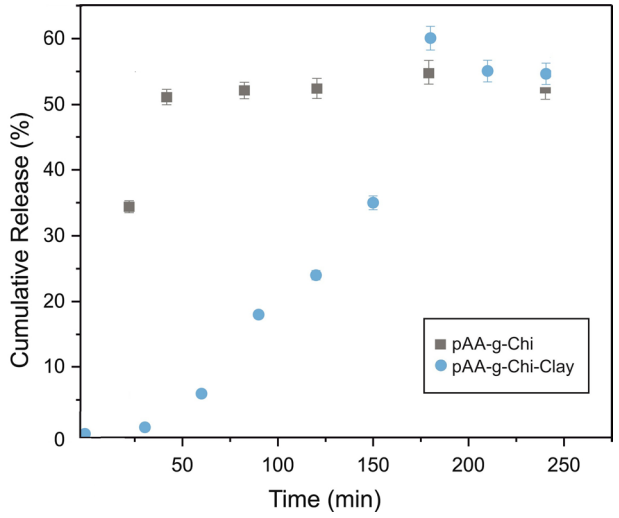

Fig. 10 Drug release in distilled water at 37 °C

Release studies of the drug active agent

To compare the dependence of drug release performance on time, the release of the pantoprazole was also investigated at two different temperatures, at 25 °C and 37 °C, and obtained results are displayed in Figs. 9 and 10, respectively.

It was observed that the drug release profiles of pAA-g-Chi-clay were more adequate for the slow release of active substance than the samples without clay. The observed release profiles indicate that the prepared pAA-g-Chi-clay produces

Table 1 Results of the kinetic constants and the linear regression values (R^2), at 25 °C

Distilled water	First-order kinetic model			Korsmeyer-Peppas kinetic model		
	R^2	K (h^{-1})	Error	R^2	K	n
pH = 6.5	0.9698	0.1839	4.6%	0.8091	1.7418	0.2925

Table 2 Results of the kinetic constants and the linear regression values (R^2), at 37 °C

Distilled water	First-order kinetic model			Korsmeyer-Peppas kinetic model		
	R^2	K (h^{-1})	Error	R^2	K	n
pH = 6.5	0.9442	0.1567	3.8%	0.9112	1.3753	0.2363

controlled and long-term drug release. In addition, the ability to provide long-term drug release gives an advantage for the absorption of the drug from the intestinal system.

From Fig. 9 it can be seen that the release of the pantoprazole from the pAA-g-Chi-clay sample in distilled water at 25 °C reached equilibrium in 210 min whereas the pAA-g-Chi sample reached in 90 min. The comparison of these release profiles at different temperatures (Figs. 9 and 10) shows a lower release at 37 °C, indicating that temperature affects the release of pantoprazole. Also, at 37 °C, the release of Pantoprazole reaches equilibrium in 180 min, which is faster than the release at 25 °C, with the latter taking (around 210 min). The first-order kinetic model and the Korsmeyer-Peppas model were used to analyze the desorption profiles of pantoprazole from the drug loaded sample pAA-g-Chi-Clay, at two different temperatures.

Tables 1 and 2 represent the kinetic values and the linear regression values (R^2) obtained from kinetic equations at 25 °C and 37 °C, respectively. The error function comparisons were used to determine the best fitting kinetic model [49, 50]. The percentage error values are also shown in the tables.

Comparing the linear regression values (R^2) of the kinetic equations, it can be seen that the release kinetics at both temperatures primarily fit the first-order kinetic model. The obtained n values at both temperatures are below 0.5, which corresponds to a Fickian diffusion mechanism. Peppas et al. have indicated that the morphology of the structure of release has a notable impact on the desorption process [43].

Conclusion

Poly(acrylic acid)-chitosan-based drug carrier with bentonite was successfully prepared and used for the pantoprazole loading and release process. The swelling properties of the prepared samples, with and without clay, were investigated. It was observed that the sample without clay has higher swelling capacity compared to one modified with clay. However, the sample containing clay showed a more stable structure. The release properties of the pantoprazole from pAA-g-Chi-clay were

analyzed using different kinetic models and the first-order model and Korsmeyer-Peppas model showed the best fit for investigated system. Experimental data on the release properties of the drug, at 25 °C and 37 °C, showed better fitting with the first-order kinetic model. The pantoprazole drug release profile also followed the Fickian diffusion mechanism (obtained n values are lower than 0.5). It has been also shown that the prepared sample is effective for loading and carrying pantoprazole, and that can be potentially used in drug delivery systems.

Acknowledgements This work was supported by the Scientific Research Fund of the Istanbul University-Cerrahpaşa. Project code: BAP-22775, and by the Ministry of Education, Science and Technological Development of the Republic of Serbia (Grant no. 451-03-9/2021-14/200134).

Author contributions All authors contributed to the study conception and design, material preparation, data collection, and analysis. The first draft of the manuscript was written by AZ Aroguz and all authors commented on previous versions of the manuscript. All authors read and approved the final manuscript.

Declarations

Conflict of interest The authors have no competing interests to declare that are relevant to the content of this article.

References

1. Yao Y, Zhou Y, Liu L et al (2020) Nanoparticle-based drug delivery in cancer therapy and its role in overcoming drug resistance. Front Mol Biosci 7:193. https://doi.org/10.3389/FMOLB.2020.00193/BIBTEX
2. Meyler's side effects of drugs - 16th Edition. https://www.elsevier.com/books/meylers-side-effects-of-drugs/aronson/978-0-444-53717-1. Accessed 6 Dec 2021
3. Giacomini KM, Krauss RM, Roden DM et al (2007) When good drugs go bad. Nat. https://doi.org/10.1038/446975a
4. Odiba A, Ukegbu C, Anunobi O et al (2016) Making drugs safer: Improving drug delivery and reducing the side effect of drugs on the human biochemical system. Nanotechnol Rev 5:183–194. https://doi.org/10.1515/NTREV-2015-0055/MACHINEREADABLECITATION/RIS
5. Tryfonidou MA, de Vries G, Hennink WE, Creemers LB (2020) "Old Drugs, New Tricks"—Local controlled drug release systems for treatment of degenerative joint disease. Adv Drug Deliv Rev 160:170–185. https://doi.org/10.1016/J.ADDR.2020.10.012
6. Li R, Peng F, Cai J et al (2020) Redox dual-stimuli responsive drug delivery systems for improving tumor-targeting ability and reducing adverse side effects. Asian J Pharm Sci 15:311–325. https://doi.org/10.1016/J.AJPS.2019.06.003
7. Rohani Shirvan A, Bashari A, Hemmatinejad N (2019) New insight into the fabrication of smart mucoadhesive buccal patches as a novel controlled-drug delivery system. Eur Polym J 119:541–550. https://doi.org/10.1016/J.EURPOLYMJ.2019.07.010
8. Qiu M, Wang D, Liang W et al (2018) Novel concept of the smart NIR-light-controlled drug release of black phosphorus nanostructure for cancer therapy. Proc Natl Acad Sci USA 115:501–506. https://doi.org/10.1073/PNAS.1714421115/-/DCSUPPLEMENTAL
9. Wu X, Liu J, Yang L, Wang F (2019) Photothermally controlled drug release system with high dose loading for synergistic chemo-photothermal therapy of multidrug resistance cancer. Colloids Surf B Biointerfaces 175:239–247. https://doi.org/10.1016/J.COLSURFB.2018.11.088
10. Aroguz AZ, Baysal K, Tasdelen B, Baysal BM (2011) Preparation, characterization, and swelling and drug release properties of a crosslinked chitosan-polycaprolactone gel. J Appl Polym Sci 119:2885–2894. https://doi.org/10.1002/app.33074
11. Gref R, Domb A, Quellec P et al (1995) The controlled intravenous delivery of drugs using PEG-coated sterically stabilized nanospheres. Adv Drug Deliv Rev 16:215–233

12. Heng PWS (2018) Controlled release drug delivery systems. Pharm Dev Technol 23:833
13. Kumar R, Mondal K, Panda PK et al (2020) Core-shell nanostructures: perspectives towards drug delivery applications. J Mater Chem B 8:8992–9027
14. Amiri M, Khazaeli P, Salehabadi A, Salavati-Niasari M (2021) Hydrogel beads-based nanocomposites in novel drug delivery platforms: recent trends and developments. Adv Colloid Interface Sci 288:102316
15. Mottaghitalab F, Farokhi M, Shokrgozar MA et al (2015) Silk fibroin nanoparticle as a novel drug delivery system. J Control Release 206:161–176. https://doi.org/10.1016/J.JCONREL.2015.03.020
16. Chou SF, Carson D, Woodrow KA (2015) Current strategies for sustaining drug release from electrospun nanofibers. J Control Release 220:584–591. https://doi.org/10.1016/J.JCONREL.2015.09.008
17. Wu J, Zhang Z, Gu J et al (2020) Mechanism of a long-term controlled drug release system based on simple blended electrospun fibers. J Control Release 320:337–346. https://doi.org/10.1016/J.JCONREL.2020.01.020
18. Mehraz L, Nouri M, Namazi H (2018) Electrospun silk fibroin/β-cyclodextrin citrate nanofibers as a novel biomaterial for application in controlled drug release. Int J Polym Mater Polym Biomater 69:211–221. https://doi.org/10.1080/00914037.2018.1552865
19. Goyanes A, Wang J, Buanz A et al (2015) 3D Printing of medicines: engineering novel oral devices with unique design and drug release characteristics. Mol Pharm 12:4077–4084. https://doi.org/10.1021/ACS.MOLPHARMACEUT.5B00510
20. Kyobula M, Adedeji A, Alexander MR et al (2017) 3D inkjet printing of tablets exploiting bespoke complex geometries for controlled and tuneable drug release. J Control Release 261:207–215. https://doi.org/10.1016/J.JCONREL.2017.06.025
21. Saadeh Y, Vyas D (2014) Nanorobotic applications in medicine: current proposals and designs. Am J Robot Surg 1:4–11. https://doi.org/10.1166/AJRS.2014.1010
22. Hu M, Ge X, Chen X et al (2020) Micro/nanorobot: a promising targeted drug delivery system. Pharmaceutics 12:1–18. https://doi.org/10.3390/PHARMACEUTICS12070665
23. Pan X, Veroniaina H, Su N et al (2021) Applications and developments of gene therapy drug delivery systems for genetic diseases. Asian J Pharm Sci. https://doi.org/10.1016/J.AJPS.2021.05.003
24. Sung YK, Kim SW (2019) Recent advances in the development of gene delivery systems. Biomater Res 231(23):1–7. https://doi.org/10.1186/S40824-019-0156-Z
25. Tewabe A, Abate A, Tamrie M et al (2021) Targeted drug delivery; from magic bullet to nanomedicine: principles, challenges, and future perspectives. J Multidiscip Healthc 14:1711–1724. https://doi.org/10.2147/JMDH.S313968
26. Benhabbour SR, Kovarova M, Jones C et al (2019) Ultra-long-acting tunable biodegradable and removable controlled release implants for drug delivery. Nat Commun 101(10):1–12. https://doi.org/10.1038/s41467-019-12141-5
27. Gomes CSF, Rautureau M, Gomes JHC, Silva EAF (2021) Interactions of clay and clay minerals with the human health. Miner latu sensu Hum Heal. https://doi.org/10.1007/978-3-030-65706-2_7
28. Nizam El-Din HM, Ibraheim DM (2021) Biological applications of nanocomposite hydrogels prepared by gamma-radiation copolymerization of acrylic acid (AAc) onto plasticized starch (PLST)/montmorillonite clay (MMT)/chitosan (CS) blends. Int J Biol Macromol 192:151–160. https://doi.org/10.1016/J.IJBIOMAC.2021.09.196
29. Selvasudha N, Dhanalekshmi U-M, Krishnaraj S et al (2020) Multifunctional clay in pharmaceuticals. Clay Sci Technol. https://doi.org/10.5772/INTECHOPEN.92408
30. García-Villén F, Carazo E, Borrego-Sánchez A, et al (2019) Clay minerals in drug delivery systems. In: Modified Clay and Zeolite Nanocomposite Materials. Elsevier, pp 129–166
31. Ghadiri M, Chrzanowski W, Rohanizadeh R (2015) Biomedical applications of cationic clay minerals. RSC Adv 5:29467–29481. https://doi.org/10.1039/C4RA16945J
32. Kaplan Can H, Şahin Ö (2015) Design, Synthesis and Characterization of 3,4-Dihydro-2H-pyran containing copolymer/clay nanocomposites. 52:465–475. https://doi.org/10.1080/10601325.2015.1029372
33. Zhao D, Yu S, Sun B et al (2018) Biomedical applications of chitosan and its derivative nanoparticles. Polym 10:462. https://doi.org/10.3390/POLYM10040462
34. Lin KF, Hsu CY, Huang TS et al (2005) A novel method to prepare chitosan/montmorillonite nanocomposites. J Appl Polym Sci 98:2042–2047. https://doi.org/10.1002/APP.22401
35. Qian L (2018) Cellulose-based composite hydrogels: preparation, structures, and applications. https://doi.org/10.1007/978-3-319-76573-0_23-1

36. Aguzzi C, Cerezo P, Viseras C, Caramella C (2007) Use of clays as drug delivery systems: possibilities and limitations. Appl Clay Sci 36:22–36. https://doi.org/10.1016/j.clay.2006.06.015
37. Surya R, Mullassery MD, Fernandez NB, Thomas D (2019) Synthesis and characterization of a clay-alginate nanocomposite for the controlled release of 5-Flurouracil. J Sci Adv Mater Devices 4:432–441. https://doi.org/10.1016/j.jsamd.2019.08.001
38. Wang Y, Wang J, Yuan Z et al (2017) Chitosan cross-linked poly(acrylic acid) hydrogels: drug release control and mechanism. Colloids Surfaces B Biointerfaces 152:252–259. https://doi.org/10.1016/J.COLSURFB.2017.01.008
39. Bashir S, Teo YY, Ramesh S et al (2018) Rheological behavior of biodegradable N-succinyl chitosan-g-poly (acrylic acid) hydrogels and their applications as drug carrier and in vitro theophylline release. Int J Biol Macromol 117:454–466. https://doi.org/10.1016/J.IJBIOMAC.2018.05.182
40. Aroğuz AZ, Teofilovic V, Budinski-Simendic JCH (2017) Highly swollen composite hydrogel for investigation of pantoprazole release profile. In: IUPAC-FAPS 2017. p 118
41. Aguilera-Castro L, Martín-de-Argila-dePrados C, Albillos-Martínez A (2016) Practical considerations in the management of proton-pump inhibitors. Rev Esp Enferm Dig 108:145–153
42. Teofilović V, Pavličević J, Erceg T et al (2021) Modification of Tokat Resadiye Bentonite with Cationic Surfactant. In: Čupić Ž (ed) Physical Chemistry 2021. The Society of Physical Chemists of Serbia, Belgrade, pp 489–491
43. Pentrák M, Hronský V, Pálková H et al (2018) Alteration of fine fraction of bentonite from Kopernica (Slovakia) under acid treatment: a combined XRD, FTIR, MAS NMR and AES study. Appl Clay Sci 163:204–213. https://doi.org/10.1016/J.CLAY.2018.07.028
44. Timofeeva MN, Panchenko VN, Krupskaya VV et al (2017) Effect of nitric acid modification of montmorillonite clay on synthesis of solketal from glycerol and acetone. Catal Commun 90:65–69. https://doi.org/10.1016/J.CATCOM.2016.11.020
45. Korsmeyer RW, Gurny R, Doelker E et al (1983) Mechanisms of solute release from porous hydrophilic polymers. Int J Pharm 15:25–35. https://doi.org/10.1016/0378-5173(83)90064-9
46. Peppas NA (1985) Analysis of Fickian and non-Fickian drug release from polymers. Pharm Acta Helv 60:110–111
47. Shaikh HK, Kshirsagar RV, Patil SG (2015) Mathematical models for drug release characterization: a review. Shaikh al World J Pharm Res 4:324
48. Mahdavinia GR, Pourjavadi A, Hosseinzadeh H, Zohuriaan MJ (2004) Modified chitosan 4. Superabsorbent hydrogels from poly(acrylic acid-co-acrylamide) grafted chitosan with salt- and pH-responsiveness properties. Eur Polym J 40:1399–1407. https://doi.org/10.1016/J.EURPOLYMJ.2004.01.039
49. Lente G (2015) Deterministic Kinetics in Chemistry and Systems Biology. Springer International Publishing, Cham
50. D'Ottone L, Ochonogor EC (2017) Error analysis of absolute rate coefficient extrapolated under pseudo-first order conditions. J Turkish Chem Soc Sect A Chem 5:29–40